POZNAN UNIVERSITY OF TECHNOLOGY ACADEMIC JOURNALS
No 99 Electrical Engineering 2019

DOI 10.21008/j.1897-0737.2019.99.0003

Wojciech MYSIŃSKI*, Bartłomiej SYSŁO*

COMPARISON BETWEEN THERMAL SIMULATION RESULTS GENERATED BY PLECS SOFTWARE AND LABORATORY MEASUREMENTS

This article deals with the subject of simulation of power losses and thermal processes occurring in semiconductors, as illustrated by an example of a DC/DC buck converter. The simulations were performed in PLECS software. The results obtained from the program were compared with measurement results of a laboratory converter model.
The physical model is based on the same components as assumed in the simulation. Similarly, the parameters of the transistor control signal were the same. During operation of the converter, the temperature changes were analyzed using a K-type thermocouple. Based on the obtained results of the temperature measurement in the steady state of the converter operation, the correctness of the simulation carried out in the PLECS program was verified and confirmed.

KEYWORDS: Thermal simulation, PLECS, buck converter, thermal time constant, IGBT, Diode, power losses.

1. INTRODUCTION

Power losses in semiconductor elements and related thermal phenomena are an important element of the design process of electronic and power electronic devices. Semiconductor manufacturers provide increasingly accurate datasheets of manufactured elements, comprising accurate equivalent thermal circuit diagrams. On the other hand, there is software available on the market that allows for efficient use of information provided by manufacturers and for determining the temperature values of individual components. One of such programs is PLECS, dedicated for power electronics devices, being a product of the Swiss company Plexim. Its distinguishing feature is the ability to combine electric, mechanical, thermal and magnetic elements in the simulation process, which allows, for example, for observing entire drive systems, including temperature changes, in which power semiconductor junctions work under given load and ambient conditions.

* Cracow University of Technology

In general, power losses in semiconductor switching components can be divided into conduction losses and switching losses [3]. In the case of an IGBT transistor, conductive losses depend on voltage drop on the conductive collector-emitter junction and on collector current:

$$P_{cond(T)} = \frac{1}{T}\int_0^{t_1} i_C(t) \cdot v_{CE}(t)dt \tag{1}$$

where:
T – transistor switching period,
t_1 – transistor conducting time,
i_C(t) – instantaneous value of collector current,
v_{CE}(t) – instantaneous value of collector-emitter voltage.

On the other hand, switching losses are provided by manufacturers as energy losses characteristics during turn-on and turn-off, dependent on the switched-off transistor collector-emitter V_{CE}, collector current of turned-on transistor I_C, junction temperature T_J and switching times, that are influenced indirectly by the value of gate resistance R_G:

$$P_{sw(T)} = f_{sw} \cdot (E_{on}(V_{CE}, I_C, T_j, R_G) + E_{off}(V_{CE}, I_C, T_j, R_G)) \tag{2}$$

where: f_{sw} – transistor switching frequency, E_{ON} – energy loss during turn-on, E_{OFF} – energy loss during turn-off.
Switching loss characteristics, provided by manufacturers for transistors with an integrated anti-parallel diode, also take into account losses from transistor tail current and reverse current of the anti-parallel diode. Therefore, no switching losses are calculated separately for the anti-parallel diode. The conduction losses for the diode are determined by the following formula:

$$P_{cond(D)} = \frac{1}{T}\int_{t_1}^{T} i_F(t) \cdot v_F(t)dt \tag{3}$$

where: i_F(t) – instantaneous value of diode forward current, v_F(t) – instantaneous value of diode forward voltage.
Total power losses can be defined as:

$$P_{tot} = P_{cond(T)} + P_{sw(T)} + P_{cond(D)} \tag{4}$$

Depending on power dissipated on semiconductor junctions, it is possible to determine the temperature at which the junctions operate, at known ambient temperature and a certain thermal resistance between the semiconductor junction and the ambient – $R_{thj\text{-}a}$. An example of a thermal model and equivalent chain of thermal resistances and capacities is shown in Figure 1.

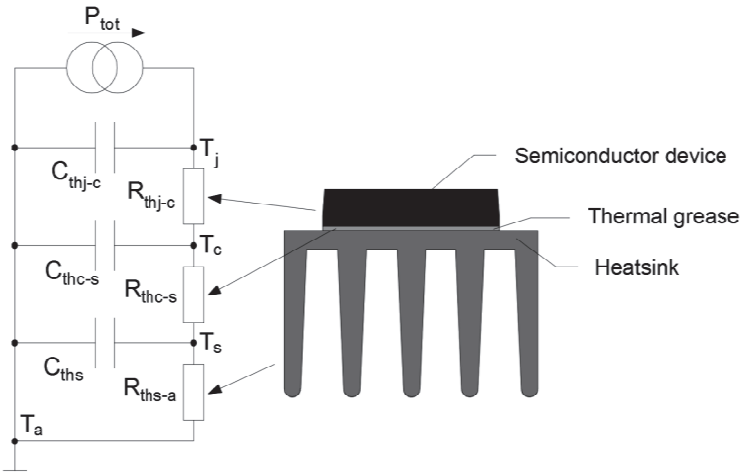

Fig. 1. Thermal model of a semiconductor device [3]

Manufacturers of semiconductor devices provide accurate information on the thermal model from the junction to the case, in the form of the Cauer or Foster thermal network [4, 5]. For a steady state, basic calculations can be carried out in accordance with formula no. 5 [2].

$$\Delta T = P_{tot} \cdot R_{th} \tag{5}$$

where:
ΔT – temperature difference,
P_{tot} – dissipated power,
R_{th} – thermal resistance.

For the case from Figure 1, it will be:

$$\Delta T_{j-a} = P_{tot} \cdot R_{thj-a} = P_{tot} \cdot (R_{thj-c} + R_{thc-s} + R_{ths-a}) \tag{6}$$

where: $R_{thj\text{-}c}$ – junction to case thermal resistance, $R_{thc\text{-}s}$ – case to heat sink thermal resistance (influence of thermal grease or pad), $R_{ths\text{-}a}$ – heat sink to ambient temperature (generally defined in heat sink datasheet).
Due to the comparative aim of this article, it was decided to select the simplest possible power electronics system so that the phenomena occurring in it are well known, and so that it is simple in practical implementation. For this reason, a DC/DC buck converter [1] was chosen, with a voltage-type input circuit and current-type output circuit. It is also the basic configuration in which the switching characteristics for power transistors are determined, including the IGBT transistors used in this experiment [6]. In the configuration used, both the switching transistor and the freewheeling diode are based on the same subassembly that is an ON Semiconductor NGTB25N120FL3WG. However, due to the lack of a stabilized high-voltage DC source with sufficient current efficiency,

it was decided to supply the measurement system using a variable autotransformer and a single-phase bridge rectifier. The measurement and simulation circuit is presented in Figure 2. In this application, the anti-parallel diode of transistor Q1 is constantly in the blocking state, while in the case of transistor Q2 the gate is shorted with the emitter, which prevents its switching.

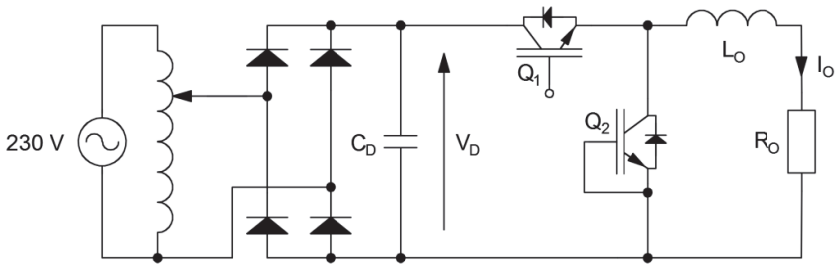

Fig. 2. Schematic of a laboratory buck converter

2. THERMAL SIMULATIONS IN PLECS

The first stage involved initial simulation of the considered system in the PLECS program, to assess the level of power losses occurring at transistors Q1 and Q2, which allowed for the selection of heat sink $R_{ths\text{-}a}$ at a level that achieves sufficient temperature, and at the same time prevents the junctions of transistors Q1 and Q2 from overheating during measurements.

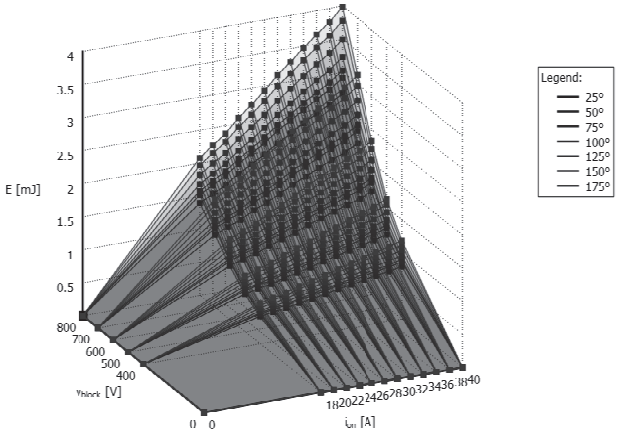

Fig. 3. Turn-on energy losses characteristics of NGTB25N120FL3WG transistor

To enter the transistor model with the integrated anti-parallel diode NGTB25N120FL3WG, the characteristics listed in the datasheet should be tabulated. To determine the losses during switching the transistor on and off, the

characteristics $E_{ON,OFF}$ = f(U_{CE}) and $E_{ON,OFF}$ = f(I_C) for different transistor junction temperatures need to be entered in a lookup table. To determine conduction losses, characteristics U_{CE} = f(I_C) for different transistor junction temperature should be entered. In order to determine conduction losses of the diode, we proceed in the same way, entering the characteristics U_f = f(I_f) for different diode junction temperature. As mentioned earlier, no separate diode switching loss characteristics are introduced in the case of a transistor with an anti-parallel diode datasheet. Examples of characteristics are shown in Figures 3 and 4.

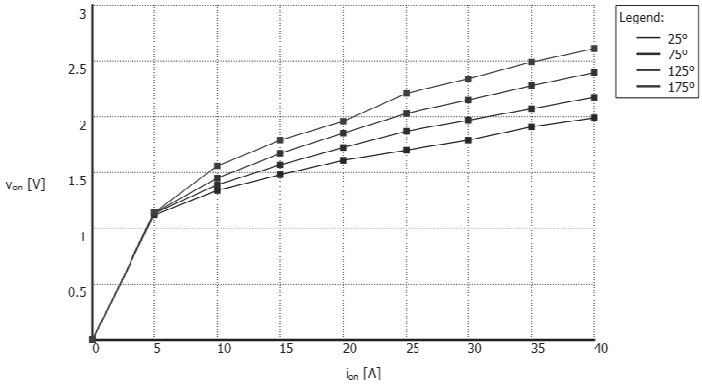

Fig. 4. Output characteristics of NGTB25N120FL3WG transistor

The equivalent thermal chain models of both the transistor and the diode should also be determined. The individual elements of the thermal network are described in detail in the datasheet. The simulation scheme in the PLECS program is presented in Figure 5.

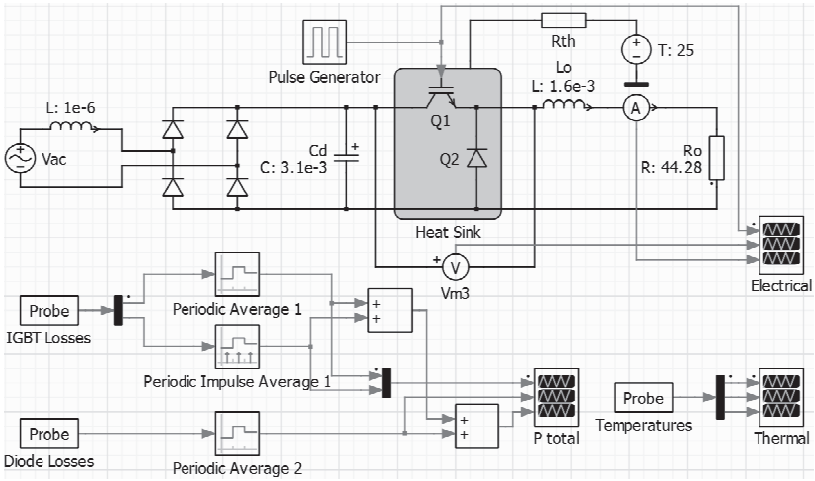

Fig. 5. Simulation schematic in PLECS

Based on the known capabilities of the bench instruments, the parameters of the laboratory system were experimentally selected so that the thermal phenomena were dynamic enough. The laboratory model uses an A5723/3 heat sink, made of aluminum alloy A6060, with a known thermal resistance specified by the manufacturer, equal to 3.7 K/W. The thermal resistance of the thermal pads under the transistors was also taken into account at 0.4 K/W (used for electrical insulation purposes). The parameters of the simulated circuit are as follows:

$$V_{ac} = \frac{300}{\sqrt{2}}\,V,\ C_D = 3.1\ mF,\ L_O = 1.6\ mH,\ R_O = 44.28\ \Omega,\ f_S = 10\ kHz,$$

$$R_{thc-s} = 0.4\,\frac{K}{W},\ R_{ths-a} = 3.7\,\frac{K}{W},\ T_a = 25\ ^oC,\ DC_{(T)} = 0.5$$

Figures 6-8 show the simulation results.

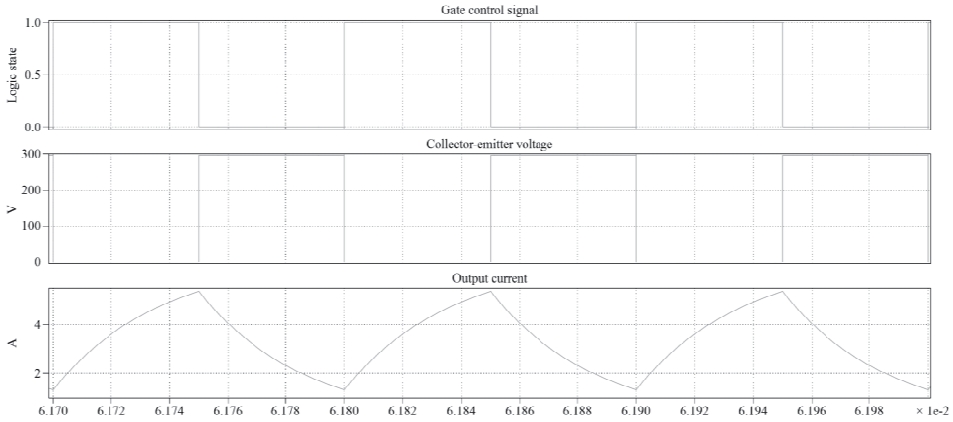

Fig. 6. Voltage and current waveforms of buck converter

The simulation of thermal phenomena requires a substantial amount of time and data memory, so it was decided to use the Steady-State Analysis option to determine the temperature of the components in the steady state. Nevertheless, with the appropriate hardware capabilities, it is possible to simulate the entire heating process of the system up to a steady state.

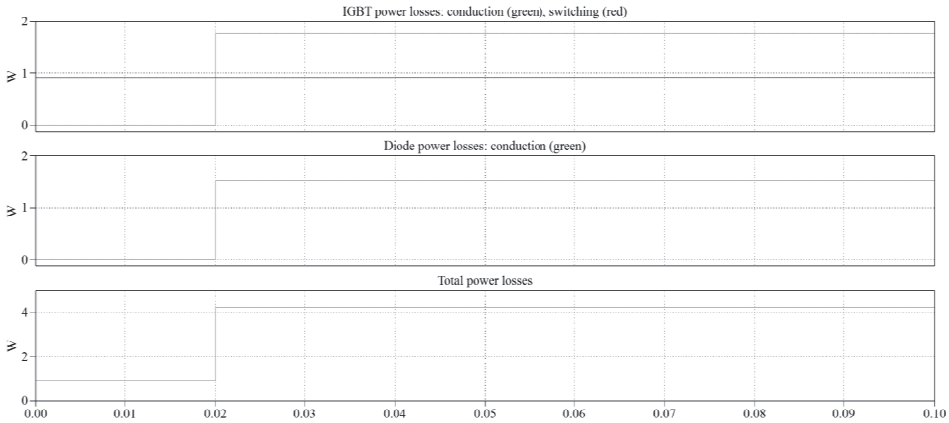

Fig. 7. Power losses – Steady state analysis

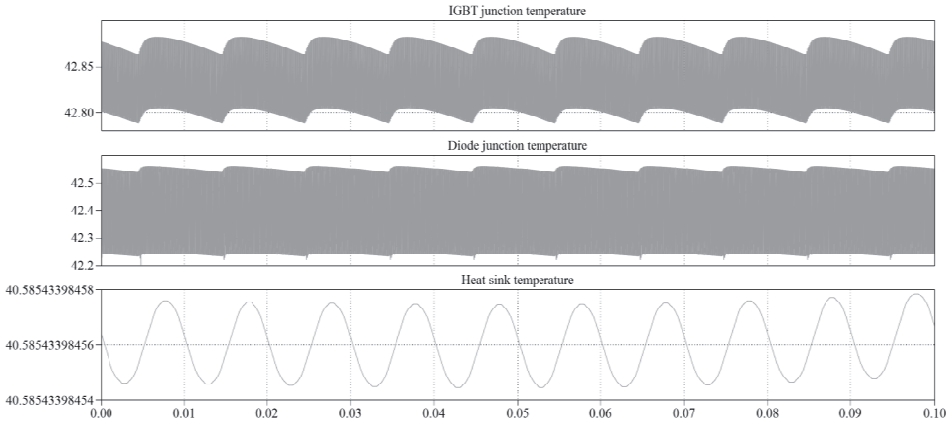

Fig. 8. Junctions and heat sink temperatures – Steady state analysis

3. VERIFICATION OF POWER LOSSES CALCULATION

In order to verify the correctness of the conducted simulations, based on the formulas introduced in the literature [3] for the buck converter, power losses occurring on semiconductors were calculated independently.

$$P_{cond(T)} = (I_{OUT} \cdot (V_{CE0(25^oC)} + TC_V \cdot (T_j - 25^oC)) + \\ + {I_{out}}^2 \cdot (r_{CE(25^oC)} + TC_r \cdot (T_j - 25^oC))) \cdot DC_{(T)} \tag{7}$$

$$P_{sw(T)} = f_{sw} \cdot E_{on+off} \cdot \left(\frac{I_{out}}{I_{ref}}\right)^{Ki} \cdot \left(\frac{V_{in}}{V_{ref}}\right)^{Ki} \cdot (1 + TC_{Esw} \cdot (T_j - T_{ref})) \tag{8}$$

$$P_{cond(D)} = (I_{OUT} \cdot (V_{F0(25^oC)} + TC_V \cdot (T_j - 25^oC)) + \\ + {I_{out}}^2 \cdot (r_{F(25^oC)} + TC_r \cdot (T_j - 25^oC))) \cdot DC_{(D)} \tag{9}$$

$$DC_{(D)} = 1 - DC_{(T)} \tag{10}$$

where: I_{OUT} – average load current, $DC_{(T)}$, $DC_{(D)}$ – transistor/diode duty cycle, TC_V, TC_r – temperature coefficients of the on-state characteristic, I_{ref}, V_{ref}, T_{ref} – reference values (datasheet), K_i – exponents for the current-dependency of switching losses (T:1, D:0.6), K_v – exponents of voltage-dependency of switching losses (T:1.35, D:0.6), TC_{Esw} – Temperature coefficients of the switching losses (0.003), TC_{Err} – temperature coefficients of the diode switching losses (0.006).
The table below shows a comparison of calculated power losses with simulation. Temperatures are calculated referring to formula 6. Junction to case thermal resistances of IGBT and anti-parallel diode are: $R_{thj\text{-}c(T)} = 0.43$ K/W, $R_{thj\text{-}c(D)} = 0.78$ K/W.

Table 1. Comparison of results obtained from simulation and formulas.

	Power losses				Temperature		
	Transistor		Diode	Total	IGBT	Diode	Heatsink
	Conduction	Switching	Conduction		$T_{j(T)}$	$T_{j(D)}$	T_s
Simulation	1.77 W	0.92 W	1.52 W	4.21 W	42.9 °C	42.5 °C	40.6 °C
Formulas	1.69 W	0.89 W	2.31 W	4.89 W	44.2 °C	44.9 °C	43.1 °C

As shown in Table 1, there are slight discrepancies between the results of simulations and calculations. These differences may be a result of different methods of using data from datasheets, inaccuracies in the selection of factors for the calculation method, as well as from the fact that not all parameters in the datasheet are well described for small currents. Generally, the convergence of results can be considered acceptable.

4. LABORATORY MODEL MEASUREMENTS

The final stage is to examine the laboratory model. The power circuit is based on the mentioned NGTB25N120FL3WG transistors, connected in a configuration such as shown in the schematic in Figure 1. All circuit parameters are the same as in the case of PLECS simulations (chapter 2).
The transistor Q1 is driven with an isolated gate driver based on the STGAP2S [7] IC. Control pulses are generated using a digital waveform generator. A differential probe was used to measure collector-emitter voltage, while the current probe was used to measure the load current. The temperature of the heat sink was also measured by a K-type thermocouple contacting the heat sink, addition-

ally secured with a special thermo-conducting adhesive: AG Termoglue. A multimeter together with an optical communication interface was used for temperature acquisition, the data was processed in dedicated software. The thermocouple was affixed between the transistors, as shown in Figure 9. The measuring bench is shown in Figure 10.

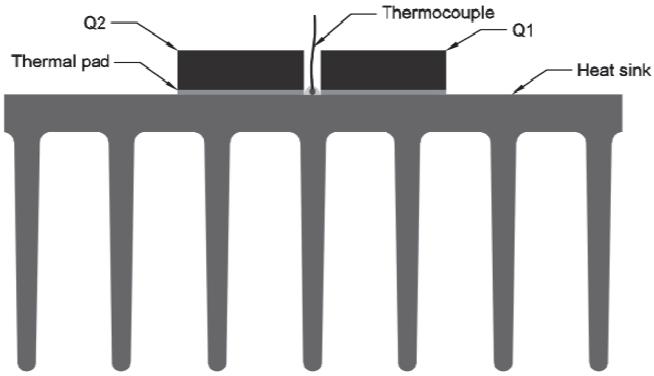

Fig. 9. Drawing of the laboratory model of buck converter power circuit

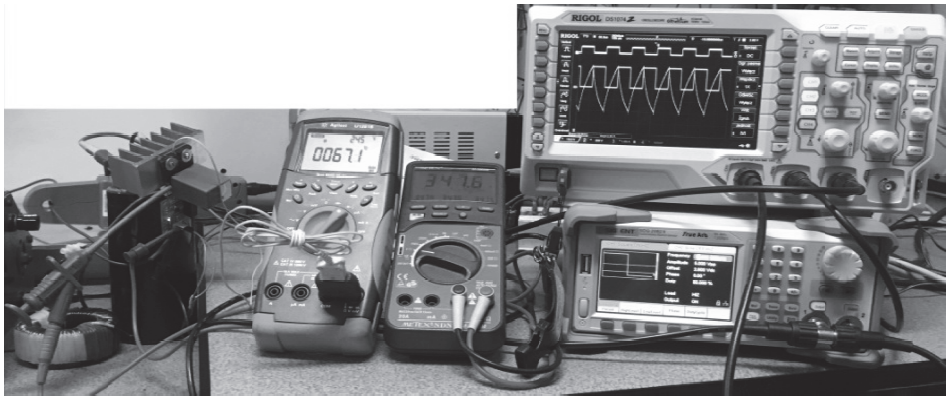

Fig. 10. Photo of measuring stand

The measurements were carried out at an ambient temperature of approx. 25°C. Below are examples of recorded waveforms. Based on several measurements, it was experimentally determined that the heat sink reaches its steady-state temperature after ca. 30 minutes. For the case under consideration, i.e. at f_s = 10 kHz, $DC_{(T)}$ = 0.5, V_D = 300 V, the heat sink temperature reached 58°C. Figures 11 and 12 present the results of one of the measurements.

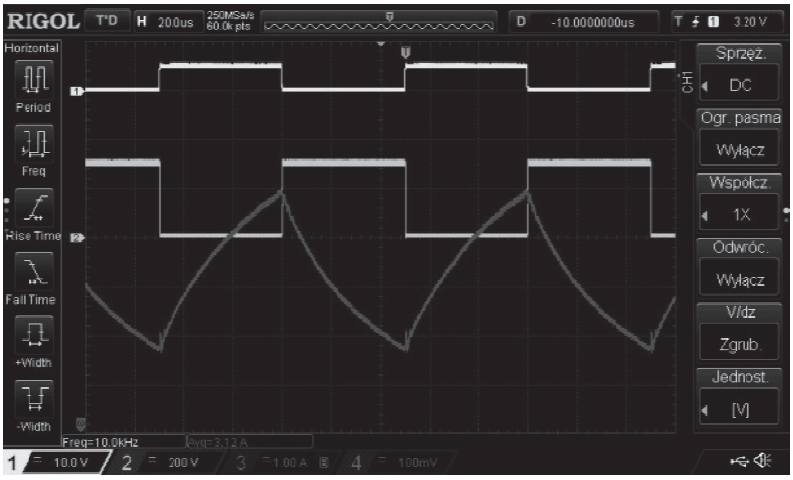

Fig. 11. Yellow – Q1 control signal, blue – Q1 collector-emitter voltage, pink – output current, at f_s = 10kHz, $DC_{(T)}$ = 0.5, V_{acA}=300 V

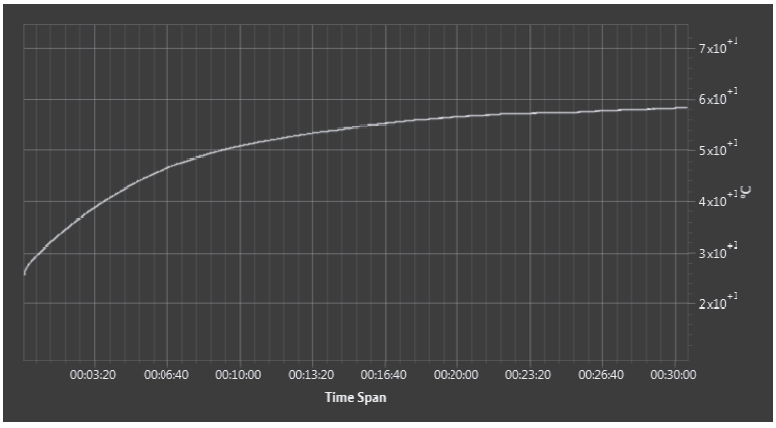

Fig. 12. Heat sink temperature

5. INTERPRETATION OF RESULTS

There is a large discrepancy between the temperature of the heat sink obtained on the basis of PLECS simulation (40.6°C) and the temperature obtained on the basis of measurements (58.3°C). Undoubtedly, what contributed to this phenomenon is the fact that the thermal resistance of the heat sink ($R_{ths\text{-}a}$) given by the manufacturers is approximate. In practice, this is not a constant parameter, it depends, among other things, on the orientation of the heat sink, air flow, surface finish, as well as the dissipated power [4, 5].

To determine the thermal resistance of the heat sink under specific conditions, it is necessary to specify a thermal time constant [8].

$$\tau_{th} = R_{th} \cdot m \cdot c_s = R_{th} \cdot C_{th} \tag{11}$$

where:
τ_{th} – thermal time constant,
m – mass of the substance,
c_s – specific heat of the substance.

Assuming a simplification that the thermal capacity of the heat sink significantly exceeds the thermal capacity of the other elements (as well as thermal resistances), based on the heat sink's time constant with the known thermal capacity, its thermal resistance was calculated.
The thermal time constant of the heat sink under is determined graphically at the level τ_{th} = 457 s. Specific heat of A6060 aluminum alloy is: c_s = 898 J/(kg·K). The mass of the heat sink with assembly screws is: m = 78 g.

$$R_{th} = \frac{\tau_{th}}{m \cdot c_s} = \frac{457}{78 \cdot 10^{-3} \cdot 898} = 6.52 \frac{K}{W} \tag{12}$$

The calculated thermal resistance significantly exceeds the value assumed in simulations (3.7 K/W). Table 2 shows the comparison of simulation results in PLECS with real measurements, taking into account indicatively determined sink-ambient thermal resistances.

Table 2. Temperature comparison between PLECS simulation and laboratory model after independent $R_{ths\text{-}a}$ correction.

R_o =44.28 Ω, L_o = 1.6mH, C_D = 3.1mF	$I_{o\ Avg}$ [A]	Corrected $R_{ths\text{-}a}$ [K/W]	Heat sink temperature [°C]	
Conditions			PLECS simulation	Measurements
f_s = 10kHz, $DC_{(T)}$ = 0.5, $V_{ac\ Amp}$=300 V	3.12	6.52	52.5	58.3
f_s = 5kHz, $DC_{(T)}$ = 0.5, $V_{ac\ Amp}$=300 V	3.25	6.44	50.4	52.9
f_s = 20kHz, $DC_{(T)}$ = 0.5, $V_{ac\ Amp}$=300 V	3.26	6.47	58.1	69.4
f_s = 10kHz, $DC_{(T)}$ = 0.1, $V_{ac\ Amp}$=300 V	**0.63**	7.90	28.4	35.3
f_s = 10kHz, $DC_{(T)}$ = 0.9, $V_{ac\ Amp}$=300 V	**5.65**	5.75	77.5	77.4
f_s = 10kHz, $DC_{(T)}$ = 0.5, $V_{ac\ Amp}$=250 V	2.57	6.60	44.4	49.9
f_s = 10kHz, $DC_{(T)}$ = 0.5, $V_{ac\ Amp}$=350 V	3.92	6.62	61.6	67.7

6. CONCLUSIONS

As shown in Table 2, there are some discrepancies between the measurements of the real system and the simulations in the PLECS program, nevertheless the correlation is quite good.

The simulation results are in most cases slightly understated, which is most likely the effect of inaccurately determining the characteristics of losses during switching and conduction for small currents in the datasheets, they were approximated in this interval (Figure 3, 4). An excellent confirmation is the measurement at f_s = 10 kHz, $DC_{(T)}$ = 0.9, $V_{ac\ Amp}$ = 300 V, in which the discrepancy between the PLECS simulation and the measurement, taking into account the correct thermal resistance of $R_{ths\text{-}a}$, is only 0.1°C. Then, the average output current was at the level of 5.65 A, which was the highest achieved value. To confirm this verdict – the greatest differences occurred at f_s = 10 kHz, $DC_{(T)}$ = 0.1, $V_{ac\ Amp}$ = 300 V, when the average output current was at the level of only 0.63 A. Better accuracy of measurements can be obtained by conducting tests in a thermal chamber to eliminate the instability of external conditions such as temperature and air flow. Nevertheless, the simulation results in PLECS presented in this article and measurements of the actual model confirm good convergence between results and provide valuable proof of the usability of PLECS simulations.

REFERENCES

[1] Rashid, Muhammad H., Power Electronics Handbook. San Diego, Academic Press, 2001.
[2] Nowak M., Barlik R., Rąbkowski J., Poradnik inżyniera energoelektronika 2. Warszawa, WNT, 2014.
[3] Wintrich A., Ulrich N., Werner T., Reimann T., Application Manual, Power Semiconductors. Nuremberg: Semikron, 2015.
[4] Górecki K., Zarębski J., The influence of the selected factors on transient thermal impedance of semiconductor devices, 2014 Proceedings of the 21st International Conference Mixed Design of Integrated Circuits and Systems (MIXDES), Lublin, 2014, pp. 309–314.
[5] Gorecki K., Zarebski J., Nonlinear Compact Thermal Model of Power Semiconductor Devices, in IEEE Transactions on Components and Packaging Technologies, vol. 33, no. 3, pp. 643–647, Sept. 2010.
[6] ON Semiconductor, IGBT, Ultra Field Stop, NGTB25N120FL3WG datasheet, Rev. 5, 2017.
[7] STMicroelectronics, Galvanically isolated 4 A single gate driver, STGAP2S datasheet, June 2018.
[8] Szekely V., Rencz M., Thermal dynamics and the time constant domain, in IEEE Transactions on Components and Packaging Technologies, vol. 23, no. 3, pp. 587–594, Sept. 2000.

(Received: 04.02.2019, revised: 05.03.2019)